Published online 27 June 2012 *Nucleic Acids Research, 2012, Vol. 40, No. 17* ***8607–8621***
doi:10.1093/nar/gks623

Identification and analysis of hepatitis C virus NS3 helicase inhibitors using nucleic acid binding assays

Sourav Mukherjee[1], Alicia M. Hanson[1], William R. Shadrick[1], Jean Ndjomou[1], Noreena L. Sweeney[1], John J. Hernandez[1], Diana Bartczak[1], Kelin Li[2], Kevin J. Frankowski[2], Julie A. Heck[3], Leggy A. Arnold[1], Frank J. Schoenen[2] and David N. Frick[1,*]

[1]Department of Chemistry and Biochemistry, University of Wisconsin-Milwaukee, Milwaukee, WI 53211, [2]University of Kansas Specialized Chemistry Center, University of Kansas, 2034 Becker Dr., Lawrence, KS 66047 and [3]Department of Biochemistry and Molecular Biology, New York Medical College, Valhalla, NY 10595, USA

Received March 26, 2012; Revised May 30, 2012; Accepted June 4, 2012

ABSTRACT

Typical assays used to discover and analyze small molecules that inhibit the hepatitis C virus (HCV) NS3 helicase yield few hits and are often confounded by compound interference. Oligonucleotide binding assays are examined here as an alternative. After comparing fluorescence polarization (FP), homogeneous time-resolved fluorescence (HTRF®; Cisbio) and AlphaScreen® (Perkin Elmer) assays, an FP-based assay was chosen to screen Sigma's Library of Pharmacologically Active Compounds (LOPAC) for compounds that inhibit NS3-DNA complex formation. Four LOPAC compounds inhibited the FP-based assay: aurintricarboxylic acid (ATA) (IC_{50} = 1.4 μM), suramin sodium salt (IC_{50} = 3.6 μM), NF 023 hydrate (IC_{50} = 6.2 μM) and tyrphostin AG 538 (IC_{50} = 3.6 μM). All but AG 538 inhibited helicase-catalyzed strand separation, and all but NF 023 inhibited replication of subgenomic HCV replicons. A counterscreen using *Escherichia coli* single-stranded DNA binding protein (SSB) revealed that none of the new HCV helicase inhibitors were specific for NS3h. However, when the SSB-based assay was used to analyze derivatives of another non-specific helicase inhibitor, the main component of the dye primuline, it revealed that some primuline derivatives (e.g. PubChem CID50930730) are up to 30-fold more specific for HCV NS3h than similarly potent HCV helicase inhibitors.

INTRODUCTION

All cells and viruses need helicases to read, replicate and repair their genomes. Cellular organisms encode numerous specialized helicases that unwind DNA, RNA or displace nucleic acid binding proteins in reactions fuelled by ATP hydrolysis. Small molecules that inhibit helicases would therefore be valuable as molecular probes to understand the biological role of a particular helicase, or as antibiotic or antiviral drugs (1,2). For example, several compounds that inhibit a helicase encoded by herpes simplex virus (HSV) are potent drugs in animal models (3,4). Despite this clear need, relatively few specific helicase inhibitors have been reported, and the mechanisms through which the most potent compounds exert their action are still not clear. Although HSV helicase inhibitors have progressed furthest in pre-clinical trials (5), the viral helicase that has been most widely studied as a drug target is the one encoded by the hepatitis C virus (HCV). The uniquely promiscuous HCV helicase unwinds duplex DNA and RNA in a reaction fuelled by virtually any nucleoside triphosphate (6). The ability of HCV helicase to act on DNA is particularly intriguing because the HCV genome and replication cycle are entirely RNA-based. There is no convincing evidence that HCV helicase ever encounters DNA in host cells. Compounds that disrupt the interaction of the helicase and DNA, therefore, would be useful to understand why an RNA virus encodes a helicase that acts on DNA. They also might be useful antivirals because HCV needs a functional helicase to replicate in cells (7) and helicase inhibitors halt HCV replication in cells (8).

*To whom correspondence should be addressed. Tel: +1 414 229 6670; Fax: +1 414 229 5530; Email: frickd@uwm.edu
Present address:
Julie A. Heck, Department of Biology, College of Wooster, Wooster, OH 44691, USA.

The HCV helicase resides in the C-terminal two-thirds of the viral multifunctional non-structural protein 3 (NS3), which is also a protease. The NS3 protease and helicase are covalently associated during HCV replication for unknown reasons. HCV and related viruses encode the only proteins known that are both proteases and helicases. Recombinant DNA technology can be used to separate the two NS3 functional domains, and express the proteins separately in *Escherichia coli* or other model organisms. Both mono-functional, recombinant, truncated NS3 proteins (called NS3p and NS3h) retain their activities *in vitro*. Although NS3h retains a helicase function, its ability to unwind RNA is somewhat diminished (9). The NS3 helicase was one of the first HCV enzymes to be characterized, and crystal structures of NS3h were first solved in the mid 1990s (10,11). However, helicase inhibitor development has been far slower than it has been for other HCV drug targets (2,12). To date, only a few classes of helicase inhibitors have been reported to slow HCV RNA replication in cells. HCV helicase inhibitors reported to act as antivirals include nucleoside mimics (13), triphenylmethanes (14), acridones (8,15), amidinoanthracyclines (16), tropolones (17), symmetrical benzimidazoles (18–20) and primuline derivatives (21).

One reason that so few molecular probes targeting HCV helicase are available is because high throughput screens for helicase inhibitors yield few hits. For example, a sensitive molecular beacon-based helicase assay (MBHA) (22) has been used to screen 290 735 compounds in the NIH Molecular Libraries Small Molecule Repository by the Scripps Research Institute Molecular Screening Center (PubChem Project: http://pubchem.ncbi.nlm.nih.gov/assay/assay.cgi?aid=1800, 14 June 2011, date last accessed), and only 500 compounds (0.2%) were confirmed as hits upon retesting (PubChem Project: http://pubchem.ncbi.nlm.nih.gov/assay/assay.cgi?aid=1943, 14 June 2011, date last accessed). The most potent hits in the NIH screen did not, however, directly inhibit helicase action, but instead they interfered with the assay (PubChem Project: http://pubchem.ncbi.nlm.nih.gov/assay/assay.cgi?aid=485301, 14 June 2011, date last accessed). They also did not inhibit HCV replication in cells (PubChem Project: http://pubchem.ncbi.nlm.nih.gov/assay/assay.cgi?aid=463235, 14 June 2011, date last accessed) (23).

Screens for helicase inhibitors typically rely on assays that monitor either helicase catalyzed strand separation or ATP hydrolysis. Both assays are relatively complex, and inhibitory compounds might act through the enzyme, ATP, nucleic acid or other required cofactors (24). Both assays monitor a helicase's motor action, and it is possible that the protein conformational changes that take place in these assays, or some other unknown factor, obfuscates inhibitor identification in large screens. Here, we test whether simpler DNA-binding assays might be more useful for HCV helicase inhibitor discovery.

Hepatitis C virus helicase binds single stranded DNA and RNA with similar high affinities in the absence of ATP. When ATP is present, it fuels helicase movements and the subsequent separation of both DNA and RNA duplexes (25). The ability of HCV helicase to separate both DNA and RNA is intriguing because other similar enzymes typically prefer DNA or RNA and because NS3 likely never encounters DNA. The RNA virus replicates in the cytoplasm and has no DNA stage in its replication cycle. Numerous NS3 crystal structures show how the protein binds DNA (26–28) or RNA (29), both in the absence or presence of ATP analogs (28,29). These structural studies reveal that amino acid side chains in the NS3h nucleic acid binding cleft do not directly contact the 2′-hydroxyl of RNA, explaining the enzyme's unusual promiscuity, and justifying the use of DNA oligonucleotides as surrogates for RNA to probe the enzyme's functions. HCV helicase binds nucleic acids with low nanomolar affinity (30,31) and NS3h preferentially interacts with polypyrimidine tracts like those found in the 3′ untranslated region of the virus genome (10,32). While it is clear that one strand of DNA (or RNA) binds in a cleft separating the two conserved helicase motor domains from a third helical domain, it is not clear where else on the protein nucleic acids might bind. Based on modeling studies, some groups have suggested that RNA might bind in the positively charged cleft separating the protease from the helicase (12,33), and more recent evidence suggests the protease region binds certain sequences in the internal ribosome entry site of the HCV RNA genome (34).

We show here how DNA binding assays can be used to identify new helicase inhibitors and how DNA binding assays with unrelated proteins can be used to screen a library of helicase inhibitors for specific compounds. A truncated NS3 lacking the protease domain (i.e. NS3h) is used because it is still unclear exactly how the protease region affects NS3–RNA interactions, and DNA is used here instead of more costly RNA, because the nucleic acid-binding site on NS3h does not differentiate between the DNA and RNA. First, we compare various DNA binding assays for their screening utility. Next, we use a fluorescence-polarization (FP)-based binding assay to identify three new HCV helicase inhibitors. Binding assays with the unrelated *E. coli* single-stranded DNA binding protein (SSB) are then used to reveal that the new compounds, like helicase inhibitors discovered in a prior screen of the NCI Mechanistic Set (21), are not specific for HCV helicase. In the final part of this study, we use a library of compounds derived from a scaffold identified in the prior screen (21) to show that binding assays can be used to differentiate specific inhibitors from non-specific HCV helicase inhibitors.

MATERIALS AND METHODS

Materials

DNA oligonucleotides were obtained from Integrated DNA Technologies (Coralville, IA). HCV NS3h was expressed and purified as described (6). Helicase substrates were prepared by combining DNA oligonucleotides (Integrated DNA Technologies, Coralville, IA) at a 1:1 molar ratio to a concentration of 20 μM in 10 mM Tris–HCl pH 8.5, placing in 95°C water, and allowing them to cool to room temperature for 1 h. The partially

duplex helicase substrates possessing a 3′ ssDNA tail were then purified of free oligonucleotides by mixing DNA 6:1 with 6X loading buffer (0.25% bromophenol blue, 0.25% xylene cyanol FF, 40% sucrose) and separating with 20% non-denaturing PAGE at a constant 200 V for 1 h.

Electrophoretic mobility shift assay

Binding assays containing 50 mM Tris, pH 7.4, 10% glycerol, 100 nM DNA substrate (5′-Cy5-CC TAC GCC ACC AGC TCC GTA GG–3′ annealed to 5′-GGA GCT GGT GGC GTA GG (T)20-3′) and 650 nM NS3h were incubated 20 min on ice. Following addition of indicated concentrations of thioflavine S, the binding reactions were incubated another 20 min on ice. A BioRad precast 15% polyacrylamide Tris/Borate/EDTA gel was pre-run at 4°C for 30 min at 120 V. Four microliters of each sample was loaded onto the gel. The gel was run 1 min at 200 V to allow samples to enter gel, then 40 min at 120 V. The gel was scanned on a Molecular Dynamics Storm 860 Phosphorimager.

FP-based DNA-binding assay

For screening, assays were performed in a total volume of 20.2 µl in 384-well, flat-bottom, low volume, black microplates (Greiner Bio-One, catalog #784076). First, 20 µl of a FP-assay solution (5 nM Cy5-TTTTTTTTTTTTTTT-3′ (Cy5-dT15), 15 nM NS3h, 25 mM MOPS, pH 7.5, 1.25 mM $MgCl_2$, 0.0025 mg/ml BSA, 0.005% (v/v) Tween20 and 0.025 mM DTT) was dispensed in each well, then 0.2 µl of dimethylsulfoxide (DMSO) or compound dissolved in DMSO was added by pin transfer, such that the final concentration of DMSO was 1% (v/v) in each assay.

For confirmation and IC_{50} value determination, assays were performed in half area 96-well microplates (Corning Life Sciences, catalog #3694). First, 47.5 µl of a FP-assay solution was dispensed in each well, then 2.5 µl of DMSO or compound dissolved in DMSO was added, such that the final concentrations in each assay were 5 nM Cy5-dT15, 15 nM NS3h, 25 mM MOPS, pH 7.5, 1.25 mM $MgCl_2$, 0.0025 mg/ml BSA, 0.005% (v/v) Tween20, 0.025 mM DTT and 5% DMSO (v/v).

Polarization was monitored with a TECAN Infinite M1000 PRO multi-mode microplate reader by exciting at 635 nm (5 nm bandwidth) and measuring total fluorescence intensity, parallel and perpendicular polarized light at 667 nm (20 nm bandwidth). G-factors were calculated from wells with Cy5-dT15 alone. Inhibition (%) was calculated by normalizing data to values obtained with positive controls (200 nM dT20 or 100 µM primuline) and negative controls (DMSO only). Assay interference was calculated by dividing fluorescence intensity of a compound-containing assay (F_c) by the average fluorescence intensity of the negative controls ($F_{(-)}$). Similar results were obtained with both assay formats as long as DMSO concentrations remained below 5%.

Compounds in the HCV helicase inhibitor library were either purchased (Sigma, St. Louis, MO) or synthesized as described (21) and screened at 20 µM. Samples in Sigma's Library of Pharmaceutically Active Compounds (LOPAC) were screened at 100 µM.

Homogeneous time resolved fluorescence (HTRF®) assay

Assays were performed in 20.2 µl in 384-well, flat-bottom, small volume, white microplates (Greiner Bio-One, catalog #784075). The procedure was the same as that for the FP assay except that 15 µl of the reaction mixtures (7.5 nM Cy5-dT15 DNA, 50 nM NS3h, 25 mM Tris, pH 7.5, 1.25 mM $MgCl_2$, 0.05 mg/ml BSA, 0.1% (v/v) Tween20, and 0.5 mM DTT) was first dispensed in each well before the addition of 0.2 µl of dT20 or H_2O. After addition, 5 µl of a (1:50 dilution) of Lumi4®-Tb Cryptate-conjugated anti-6 Histidine mouse monoclonal antibody (catalog #61HISTLA, CISBIO US) was added and the plate was incubated for 60 min at 4°C. TR-FRET was monitored with a Fluostar Omega multimodal plate reader (BMG Labtech, Inc.) by excitation of the donor fluorophore at 340 nm. TR-FRET ratio was calculated as emission of acceptor fluorophore at 665 nm over the emission of donor fluorophore at 620 nm (gain 2300, integration time 400 µs, integration start time 60 µs, positioning delay 0.2 s, measurement start time 0 s, number of flashes per well 200).

AlphaScreen® assay

All assays were similar to the above assays except that they contained a final concentration of 10 nM biotinylated oligonucleotide (Bio-d18, 5′-Bio-GCC TCG CTG CCG TCG CCA-3′), instead of Cy5-dT15, and they used reagents from the AlphaScreen® Histidine (Nickel Chelate) Detection Kit (catalog #6760619C, Perkin Elmer). To 384-well, flat-bottom, low volume, white microplates (Greiner Bio-One, catalog #784075), 12 µl of the reaction mixtures containing 10 nM Bio-d18, 20 nM NS3h, 25 mM HEPES, pH 7.5, 100 mM NaCl and 1.0 mg/ml BSA was dispensed, followed by 0.2 µl of dT20 or H_2O and 4 µl Anti-His alpha screen donor beads. After incubation for 30 min at 23°C, 4 µl of streptavidin-acceptor beads was added, and the assays incubated another 60 min. All work with the alpha reagents was performed under green filtered light conditions (<100 Lux). Alpha counts were measured at 520–620 nm (Ex. 680 nm, 20 nm bandwidth) in a Fluostar Omega multimodal plate reader (BMG Labtech, Inc.).

NS3h MBHAs

The ability of compounds to inhibit helicase action was monitored using molecular beacons as described previously (19,22). Assays contained 25 mM MOPS, 1.25 mM $MgCl_2$, 5% DMSO, 5 µg/ml BSA, 0.01% (v/v) Tween20, 0.05 mM DTT, 5 nM substrate, 12.5 nM NS3h and 1 mM ATP. The partially duplex DNA substrates used in MBHAs consisted of a 45-mer bottom strand 5′-GCT CCC CGT TCA TCG ATT GGG GAG C(T)20-3′ and the 25-mer HCV top strand 5-/5Cy5/GCT CCC CAA TCG ATG AAC GGG GAG C/3IAbRQSp/-3. The 3-stranded RNA substrate used was made of two RNA strands, a 60 nucleotide long bottom strand 5′-rGrGrA rGrCrU rGrGrU rGrGrC rGrUrA rGrGrC rArArG rArGrU rGrCrC rUrUrG

rArCrG rArUrA rCrArG rCrUrU rUrUrU rUrUrU rUrUrU rUrUrU rUrUrU-3′, a 24 nucleotide long top strand 5′-rArGrU rGrCrG rCrUrG rUrArU rCrGrU rCrArA rGrGrC rArCrU-Cy5, and a third DNA top strand with the sequence/5IAbRQ/CCT ACG CCA CCA GCT CCG TAG G-3. In the screen in Figure 5, percent inhibition was calculated with equation (1) and interference with equation (2).

$$\text{Inhibition (\%)} = ((Fc_0/Fc_{30}) - (F(-)_0/F(-)_{30})/ (1 - (F(-)_0/F(-)_{30}))) \times 100 \quad (1)$$

$$\text{Interference (ratio)} = (Fc_0/F(-)_0) \quad (2)$$

In equations (1) and (2), Fc_0 is the fluorescence of the reactions containing the test compound before adding ATP, Fc_{30} is the fluorescence of the test compound reaction 30 min after adding ATP. $F(-)_0$ is the average of three DMSO-only negative control reactions before adding ATP and $F(-)_{30}$ is the average of three DMSO-only reactions 30 min after adding ATP.

To monitor helicase reaction kinetics and to calculate IC_{50} values, assays were performed in a volume of 60 µl in white half-area 96-well plates (Corning Lifesciences, catalog #3693) and measured in a Fluostar Omega multi-modal plate reader (BMG Labtech, Inc.) using the 640 nm excitation wavelength and 680 emission wavelength filters. Reactions were performed by first incubating all components except for ATP for 2 min, then initiated by injecting in 1/10 volume of ATP such that the final concentration of all components was as noted above. Initial reaction velocities were calculated by fitting a first order decay equation to data obtained after ATP addition and calculating an initial velocity from the resulting amplitude and rate constant. The concentration at which a compound causes a 50% reduction in reaction velocity (IC_{50}) was calculated using GraphPad Prism (v. 5).

HCV replicon assays

The ability of compounds to inhibit HCV replication was judged using an HCV *Renilla* luciferase (HCV RLuc) reporter construct that was a generous gift from Seng-Lai Tan (35). Plasmid DNA expressing the replicon was transcribed, and the subsequently purified RNA was used to prepare stably transfected Huh7.5 cells by prolonged selection with G418. To test compounds, HCV RLuc replicon containing cells were seeded at a density of 10 000 cells per well in 96-well plates and incubated for 4–5 h to allow the cells to attach to the plate in 100 µl of DMEM supplemented with 10% fetal bovine serum (HyClone), 2 mM L-glutamine, 100 U/ml penicillin, 100 µg/ml streptomycin and 1x non-essential amino-acids (Invitrogen). To each well, 0.5 µl of compounds dissolved in DMSO were added such that the DMSO final concentration was 0.5%, and the cells were incubated for 72 h at 37°C under 5% CO_2 atmosphere. The effect of compounds on HCV replication was estimated by measuring the *Renilla* luciferase activity using the *Renilla* luciferase assay system (Promega, Madison, WI) in 96-well black microplates (Thermo Scientific, catalog #9502867) read on a FLUOstar Omega multi-mode microplate reader (BMG Labtech, Inc.). Relative percent inhibition was calculated by normalizing values to those obtained with cells treated with DMSO only.

Cell viability assay

To assess compound toxicity towards Huh-7.5 cells, cells were plated and treated as above and viability was assessed using the Cell Titer-Glo luminescent cell viability kit (Promega) following the manufacturer's instructions. Briefly, at the end of a 72 h incubation period, the medium was removed and the cells were washed with growth medium, then an equal volume of growth medium and Cell Titer-Glo reagent was added and the lysis was initiated by mixing on an orbital shaker. The plate was incubated at 23°C for 30 min and luciferase activity was measured for 1 s using a FLUOstar Omega microplate reader (BMG Labtech, Inc.) in black 96-well microplates (Thermo Scientific, catalog #9502867). Relative viability was calculated by normalizing the values to those obtained with cells treated with DMSO only.

Escherichia coli SSB assay

The procedure for screening with this assay was the same as that for the FP-based DNA binding assay carried out in 384-well plates except that *E. coli* SSB (Promega) was used at 20 nM instead of the HCV helicase. For IC_{50} determination, assays were performed with 60 µl total volume in black flat bottomed 384-well microplates (Corning catalog #3573). First, 3.0 µl of DMSO or compound dissolved in DMSO was added, such that the final concentration of DMSO was 5% (v/v) in each assay. Then 57 µl of a FP-assay solution (5 nM Cy5-dT15, 20 nM SSB, 25 mM MOPS, pH 7.5, 1.25 mM $MgCl_2$, 0.0025 mg/ml BSA, 0.005% (v/v) Tween20 and 0.025 mM DTT) was dispensed in each well. Polarization was monitored as described above.

RESULTS

Belon and Frick (36) previously reported that thioflavine S was an HCV helicase inhibitor, and thioflavine S was used as a positive control for the screen of the NIH Molecular Libraries Small Molecule Repository (PubChem BioAssay AID #1800) and in other studies (37). While studying the mechanism of action of thioflavine S (Direct Yellow 7, Sigma Cat. #T1892) and the related yellow dyes primuline (Direct Yellow 59, MP Biomedicals Cat. #195454) and titan yellow (Direct Yellow 9/Thiazole Yellow G, Sigma Cat. #88390) (38), we observed that they prevent NS3h from binding its nucleic acid substrate (Figure 1A). In the absence of one of these dyes, NS3h binds its substrate tightly enough that the complex will migrate more slowly through a non-denaturing polyacrylamide gel. When thioflavine S was present the gel-shift of the substrate decreased in a concentration-dependent fashion (Figure 1B).

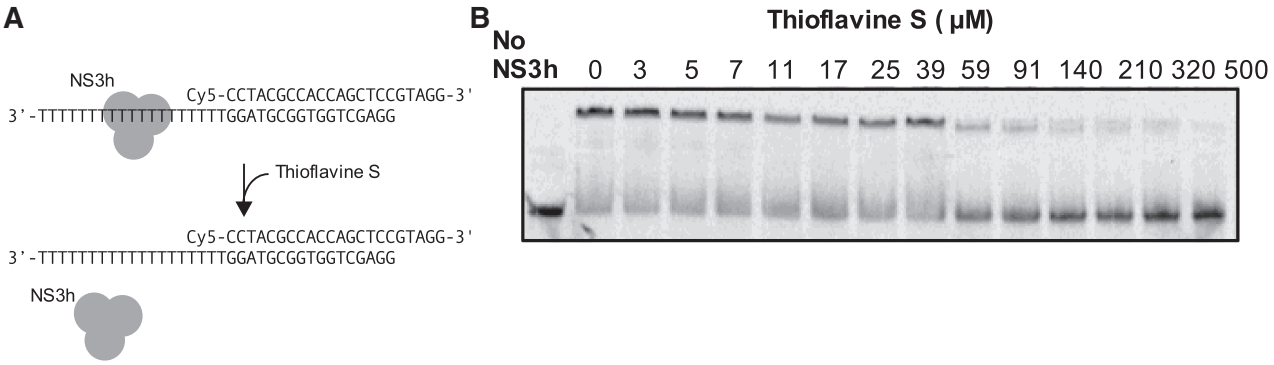

Figure 1. Thioflavine S inhibits the ability of NS3h to bind to its DNA substrate. (**A**) Partially duplex DNA helicase substrate used for gel-shift analysis. (**B**) Electrophoretic mobility shift assay (EMSA). Samples containing the MBHA substrate (100 nM), NS3h (650 nM) and indicated concentrations of thioflavine S were examined on a 15% native polyacrylamide gel using a phosphorimager to locate labeled DNA. Control lane with no NS3h shows migration position of free DNA.

HCV helicase-DNA binding assays that are suitable for high throughput screening

To unwind a substrate, HCV helicase binds a single stranded nucleic acid tail then translocates in a 3′–5′ direction (39) until it reaches a duplex region that it can separate. The ability of NS3h to bind its substrate can also be measured by monitoring changes in polarization (or anisotropy) of a fluorescent helicase substrate as has been done with related helicases (40,41). This loading step can be monitored using a truncated substrate lacking duplex regions, such as a 15-nucleotide long deoxythymidine polymer (dT15) (Figure 2A). Previous work has shown that NS3h binds such single stranded DNA with a high affinity and that 2-3 protomers bind such an oligonucleotide. A homopolymer was chosen to minimize the possibility that the DNA would form a hairpin or other secondary structures, and Ts were chosen because NS3h prefers this sequence to others (10,30–32).

As seen before (30,31,42), the binding of NS3 to DNA in this FP-assay was stoichiometric ($K_d < 1$ nM) and about two to three molecules of NS3 were needed to saturate Cy5-dT15. When 5 nM Cy5-dT15 was present, increasing amounts of NS3h increased the FP of Cy5-dT15 in a concentration dependent manner such that the amount of NS3h needed to bind half of the Cy5-dT15 ($K_{0.5}$) was 9 ± 1.5 nM. Under these conditions, the signal plateaued when about three times as much NS3h (15 nM) was added as the amount of Cy5-dT15 (Figure 2B). The polarization of a Cy5-dT15–NS3h complex decreased in the presence of either unlabeled ligand (dT20) or a yellow dye in a concentration dependent manner (Figure 2C). The IC_{50} values measured for dT20 and primuline were 7 ± 2 nM and 24 ± 3 μM, respectively. Thioflavine S decreased polarization less effectively than primuline with an IC_{50} of 35 ± 3.5 μM, and titan yellow was 10 times more potent than either with an IC_{50} value of 2.8 ± 0.2 μM (Table 1).

A Cy5-labeled oligonucleotide was chosen mainly because its fluorescence intensity did not change upon protein binding, and because it absorbs and emits light in the far-red visible range, where it would be less likely to interact with compounds in large chemical libraries. One possible problem with using Cy5 as a tracer in such a study is that it is coupled to the oligonucleotide with an aliphatic linker so that the fluorophore could, in theory, be still relatively free to rotate even when DNA is bound to the enzyme, a phenomenon commonly referred to as 'the propeller effect'. We therefore also tested oligonucleotides labeled with fluorescent moieties not bound to aliphatic linkers such as with 6-carboxyfluorescein, hexachlorofluorescein and boron-dipyrromethene (BODIPY). Polarization studies with each of these alternatives were confounded by the fact that the fluorescence intensity of each changed upon protein binding. The fact that fluorescence intensity of oligonucleotides changes when they bind the unusually acidic DNA binding site of NS3 has been previously documented (9,19). While screening fluorescent oligonucleotides, we found two other red-shifted tracers that did not change intensity upon binding, Tye^{TM} 665 and Alexa Fluor 647^{TM}. Identical (dT15) oligonucleotides labeled on the 5′-end with either Cy5, Tye665, or Alexa Fluor 647, bound NS3h with similar $K_{0.5}$s (5 ± 1, 8 ± 2 and 6 ± 2, respectively), and titan yellow inhibited complex formation of each with a similar IC_{50} value (7 ± 3, 5 ± 1 and 9 ± 4 μM, respectively). Repeated assays ($n = 40$) with the three different fluorescence tracers in the presence and absence of titan yellow (100 μM) revealed similar Z′ factors (43). Assays with Alexa Fluor and Tye 665 labeled oligonucleotides had the largest difference between the positive and negative controls, but their assay-to-assay variability was higher, particularly in assays done in the absence of inhibitor (Figure 2D). Further experiments were therefore performed with the Cy5-labeled oligonucleotide.

After optimizing conditions, FP-based binding assays were then performed in a high throughput format to judge necessary precision and reproducibility. To judge well-to-well variation, 48 negative controls (DMSO only) and 48 positive controls (100 μM primuline) were performed. The coefficient of variation was 2.2% for the negative controls and 5.8% for the positive controls, resulting in a Z′ factor of 0.81 (Figure 2E). Similar Z′ factors, and concentration response curves were obtained when plates were compared (Figure 2F) or

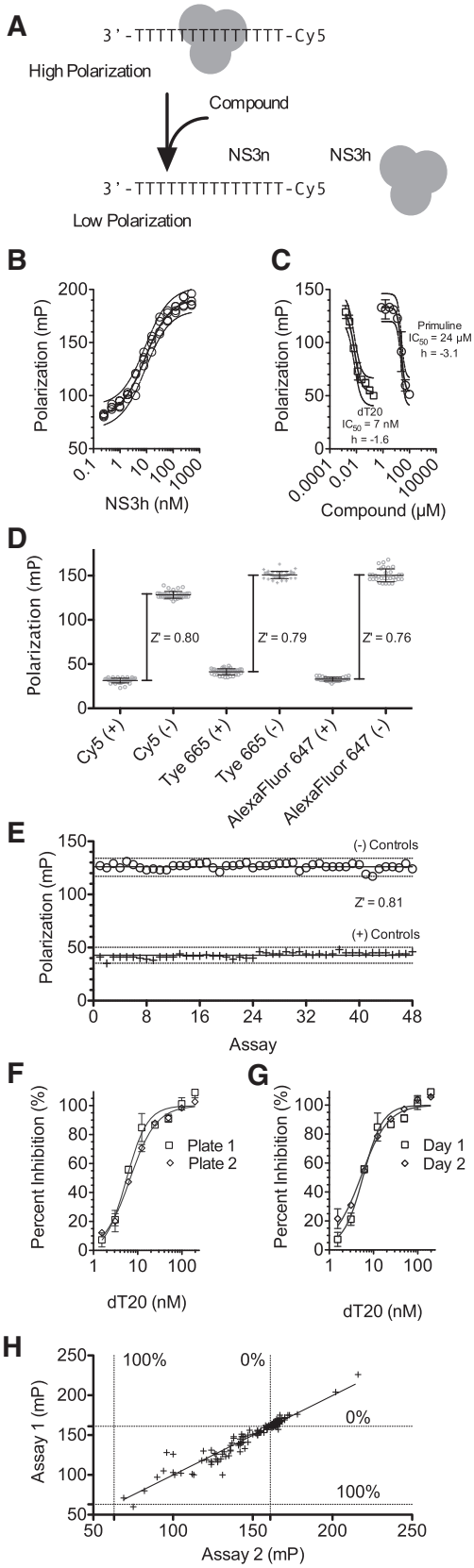

Figure 2. Fluorescence polarization (FP)-based assay to monitor the interaction of HCV helicase and a deoxythymidine polymer. (**A**) FP based assay to monitor NS3h binding to Cy5-dT15. (**B**) Fluorescence polarization of Cy5-dT15 (5 nM) at different concentrations of NS3h. Data ($n = 4$) were fitted to a concentration-response equation (four parameter, variable slope) with dotted lines showing the 95% confidence intervals for the curve fit. (**C**) Concentration response of unlabeled dT20 (squares) or primuline (circles) on the fluorescence polarization of a Cy5-dT15-NS3h complex. Data ($n = 4$) were fitted to a four-parameter concentration response equation (variable slope) constrained to values obtained in the absence of inhibitor (top) and the absence of NS3h (bottom), with indicated IC_{50} values and Hill slopes. (**D**) Comparison of results obtained with Cy5-dT15 with those obtained with dT15 labeled with either Tye665 or AlexaFluor 647. Oligonucleotides were present at 5 nM and NS3h at 15 nM. Positive controls ($N = 40$) contained 100 µM titan yellow, negative control contained DMSO only. (**E**) Fluorescence polarization of 48 positive control assays (100 µM primuline (+)) and 48 negative control assays (DMSO only (−)). Solid lines represent means and dotted lines 3 times the standard deviations of the mean of all assays. (**F**) Normalized percent inhibition of Cy5-dT15 complex formation by various concentrations of dT20 observed in FP-assays performed on two different plates. (**G**) Normalized percent inhibition of Cy5-dT15 complex formation by various concentrations of dT20 observed in FP-assays performed on two different days. (**H**) Correlation plot of fluorescence polarization values observed in duplicate assays at 20 µM of samples in an HCV helicase inhibitor library (Table S1). Data were fitted to a straight line through zero (slope = 0.97, $R^2 = 0.99$). The dotted lines show values representing 0% and 100% inhibition, as determined from negative controls (DMSO only) and positive control (100 µM primuline).

assays were performed on different days (Figure 2G). To judge reproducibility, duplicate assays were performed with 143 different HCV helicase inhibitors at a concentration of 20 µM. All but two samples in this library decreased polarization of the Cy5-dT15–NS3h complex to some extent in a reproducible fashion. Two compounds in the collection, the DNA binding dyes H33258 and TO-PRO3 (Invitrogen), increased polarization, suggesting that they bound the Cy5–DNA–NS3h complex but did not displace the oligonucleotide (Figure 2H).

Two other methods that are frequently used to monitor protein nucleic acid interactions were compared with the above FP-based assay. The first was a modified homogeneous time resolved fluorescence (HTRF®) assay (Cisbio bioassays), in which Cy5-dT15 was used as an acceptor of long-lived lanthanide fluorescence. While optimizing this TR-FRET assay, we tested three different lanthanide donors: a Lumi4®-Tb Cryptate-conjugated anti-6 Histidine mouse monoclonal antibody (catalog #61HISTLA, Cisbio), an Eu^{3+} Cryptate-conjugated mouse anti-6 Histidine monoclonal antibody (catalog #61HISKLA, Cisbio) and a LANCE® Europium Anti-6X Histidine antibody (catalog #AD0110, Perkin Elmer). The highest Z′ factors were obtained with the Tb^{3+} cryptate (data not shown). The optimized TR-FRET-based assay was performed in the same buffer as the FP-based assays, except that diluted anti-6 His antibody was added to each assay. In the HTRF® assay setup, the ratio of signals from the donor and acceptor is multiplied by 10 000 to estimate TR-FRET. In our assay, time resolved fluorescence occurring after excitation at 340 nm was measured at 625 nm, and the signal resulting from binding was detected at a wavelength of 665 nm due to energy transfer to the Cy5 (Figure 3A). The maximal energy transfer resulted in a 3.5-fold increase of the signal ratio in the presence of NS3h bound to the Tb^{3+}-conjugated anti-hexahistidine antibody. This signal change returned to baseline upon addition of

Table 1. Effects of yellow dyes and small molecules on the interaction of NS3h with DNA, its ability to unwind DNA and RNA, and HCV replication in cells

Compound	DNA binding assays[a]		NS3h helicase assays[b]		Cellular assays	
	NS3h IC_{50} (μM) ± SD	SSB IC_{50} (μM) ± SD	DNA IC_{50} (μM) ± SD	RNA IC_{50} (μM) ± SD	HCV replicon[c] IC_{50} (μM) ± SD	Viability[c] CC_{50} (μM) ± SD
Thioflavine S	35 ± 3.5	12 ± 0.9	24 ± 1.3	22 ± 6.3	>100	>100
Primuline	24 ± 3	5.0 ± 1.4	12 ± 1.3	15 ± 2.3	>100	>100
Titan yellow	2.8 ± 0.2	2.9 ± 0.2	12 ± 3.6	30 ± 3.6	>100	>100
ATA	1.4 ± 0.1	1.0 ± 0.1	0.6 ± 0.1	0.8 ± 0.2	98 ± 30	>100
AG 538	3.6 ± 0.2	1.2 ± 0.1	>100	>100	18 ± 3.2	60 ± 13
NF 023	6.3 ± 0.6	1.7 ± 0.2	2.6 ± 0.4	5.1 ± 1.2	>25[d]	>25[d]
Suramin	3.6 ± 0.3	0.3 ± 0.0	3.7 ± 0.7	8.9 ± 2.0	38 ± 9.3 [e]	>50[e]

[a]Average (±SD) IC_{50} value from three sets of FP-based binding assay performed with a 16 point 1.5-fold dilution series of each compound starting at 100 μM.
[b]Average (±SD) IC_{50} value from 3 sets of molecular beacon based helicase assays performed with a 16 point 1.5-fold dilution series of each compound starting at 100 μM.
[c]Average (±SD) IC_{50} value from three sets of assays performed with a 8 point 2-fold dilution series starting at 100 μM.
[d]Average (±SD) IC_{50} value from three sets of assays performed with a 8 point 2-fold dilution series starting at 25 μM.
[e]Average (±SD) IC_{50} value from three sets of assays performed with a 8 point 2-fold dilution series starting at 50 μM.

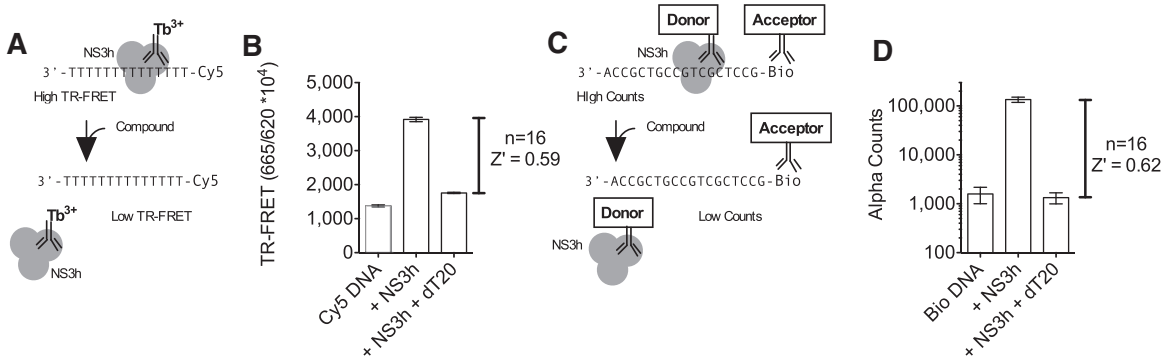

Figure 3. HTRF® and AlphaScreen® assays that detect NS3h interactions with DNA. (**A**) TR-FRET assay using the Lumi4®-Tb cryptate-conjugated anti-hexahistidine (Cisbio Bioassays) as a donor and Cy5-dT15 as an acceptor. (**B**) TR-FRET observed with 5 nM Cy5-dT15 alone, with 15 nM NS3h, and with 15 nM NS3h and 200 nM dT20. Error bars are standard deviations ($n = 16$). (**C**) Use of AlphaScreen® Histidine (Nickel Chelate) Detection Kit (Perkin Elmer) reagents to monitor NS3h binding to a biotinylated oligonucleotide. (**D**) AlphaScreen® counts for control assays containing 10 nM Bio-d18 alone, with 20 nM NS3h, and with NS3h and 200 nM dT20. Error bars are standard deviations ($n = 16$).

unlabeled oligonucleotide, dT_{20} (200 nM) (Figure 3B). Compounds that disrupt the Cy5-dT15-NS3h complex also decreased the TR-FRET signal in a concentration-dependent fashion with IC_{50} values similar to those determined with the FP-based assay (data not shown), but the Z′-factor (0.59) for the TR-FRET assay was less than what was observed with FP-based assay (Figure 3B).

The second assay compared to the FP-based assay was based on the AlphaScreen® Histidine (Nickel Chelate) Detection Kit (catalog #6760619C, Perkin Elmer). This AlphaScreen® assay monitored the binding of NS3h to DNA, using donor beads containing Ni^{2+} ions that interact with the C-terminal His-tag of NS3h and streptavidin-bound acceptor beads binding to biotinylated oligonucleotide (Bio-d18) (Figure 3C). Formation of an NS3h–DNA complex brings the donor and acceptor close enough that singlet oxygen can be transferred from the donor to acceptor beads. Compounds that disrupt the Bio-d18–NS3h complex (e.g. dT20) decrease the AlphaScreen® signal (Figure 3D). The signal/background in this AlphaScreen® was better than was seen in other assays, with the complex yielding 80- to 100-fold increased counts, but assay variability was higher than with the FP assay, leading to a Z′ factor of 0.62, which was again less than what was observed in the FP-based assay.

Compound interference and advantage over unwinding assays

Most of the compounds in the above helicase inhibitor library were previously shown to inhibit NS3h when screened using an MBHA (21). The MBHA (22) monitors the ability of a helicase to remove a molecular beacon (44) bound to a complementary strand upon ATP addition (Figure 4A). In the absence of inhibitors, fluorescence decreases in the MBHA upon ATP addition, but when an inhibitor (*e.g.* titan yellow) is present, fluorescence decreases at a slower rate (Figure 4B). The main

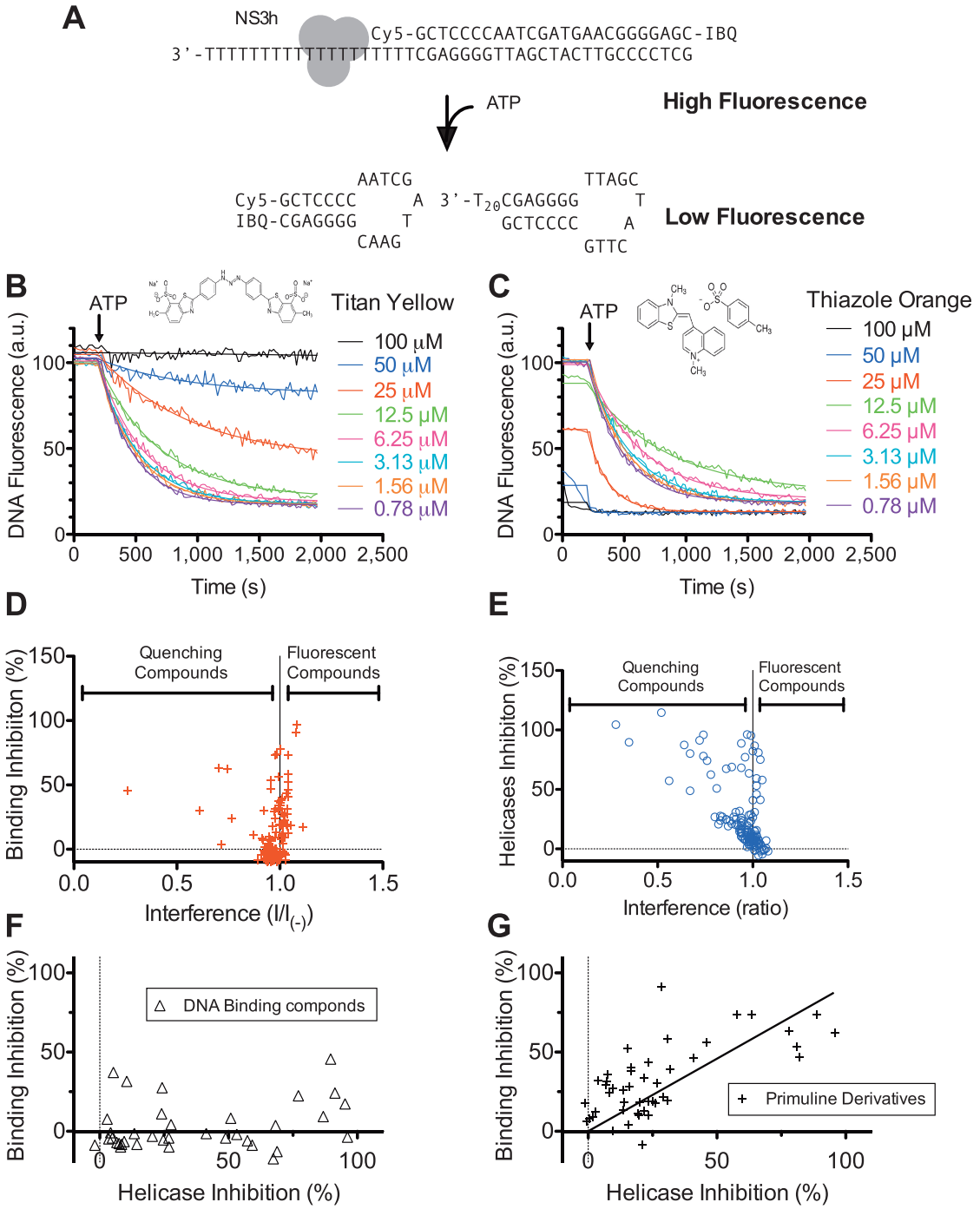

Figure 4. Comparison of HCV helicase DNA binding and unwinding assays. (**A**) The molecular beacon helicase assay (MBHA). (**B**) Effect of indicated concentrations of titan yellow on MBHAs. (**C**) Effect of indicated concentrations of thiazole orange on MBHAs. (B) and (C) show both the fluorescence traces for each reaction and the curve fits used to determine initial rates of DNA unwinding. (**D**) Mean percentage inhibition (equation (1)) and compound interference (equation (2)) of duplicate FP-based binding assays (+) performed with samples from a library of HCV helicase inhibitors. (**E**) Mean percentage inhibition (equation (1)) and compound interference (equation (2)) of duplicate MBHAs performed with samples from a library of HCV helicase inhibitors. In (D) and (E), the dotted line denotes 0% inhibition and the solid vertical line denotes no interference. (**F**) Percentage inhibition seen in the MBHA and FP-based assay for DNA binding compounds present in the library screened in panels (D) and (E). Note that most DNA-binding compounds that inhibited the MBHA screen did not inhibit the FP-binding assay. (**G**) Percentage inhibition seen in the MBHA and FP-based assay for the primuline derivatives present in the library screened in panels (D) and (E). Line shows the correlation of the ability to inhibit both unwinding and binding. Full data for both screens are in Table S1.

problem with using the MBHA, or similar unwinding assays to screen for helicase inhibitors, is that it is difficult to distinguish helicase inhibitors from compounds that simply interfere with the assay by binding DNA, such as thiazole orange (45) (Figure 4C). In screens, the ability of a compound to inhibit the MBHA is measured by comparing the fluorescence of the MBHA substrate before and after ATP addition. If a compound simply reduces fluorescence of the Cy5 substrate before ATP is added, as seen with concentrations of thiazole orange >12.5 μM (Figure 4C), it might falsely appear to inhibit the helicase. A simple method to identify true helicase inhibitors is to plot percent inhibition *vs*. compound interference, which is calculated by dividing assay fluorescence before ATP addition (F_0) by the fluorescence seen in negative control reactions ($F_{0(-)}$), which lack any inhibitory compounds (21). To compare the results of a DNA binding assay with the MBHA, the same library of known HCV helicase inhibitors, which was screened with the FP-based binding assay (Figure 4D), was re-screened with the MBHA at the same compound concentration (20 μM) (Figure 4E). When each screen was analyzed for both percent inhibition and compound interference, it was clear that fewer compounds interfered with the FP-based binding assay (Figure 4D) than with the MBHA (Figure 4E). For full results, see Table S1 (Supplementary Data). The fact that fewer compounds interfered with the FP-based assay suggests that many library samples did not decrease fluorescence by simply quenching Cy5 fluorescence.

Another way that a compound might decrease the fluorescence of the MBHA substrate would be to distort the duplex region such that the quenching moiety of the beacon is more likely to interact with the Cy5 fluorophore. If that were the case, then most DNA binding compounds should appear to inhibit the MBHA but not the FP-based binding assay, which lacks a duplex region. To test this hypothesis, the average percent inhibition observed with each compound in FP-based binding assays was compared with the average percent inhibition seen in the MBHA unwinding assay. Such a plot reveals that most of the known DNA binding compounds in our HCV helicase inhibitor library (e.g. berenil, proflavin, netropsin and SYBR green I) inhibit the MBHA but not the FP-based binding assay (Figure 4F). In contrast, compounds, which act mainly by inhibiting the ability of NS3h to bind DNA, such as those derived from primuline (21), inhibit both the FP-binding assay and MBHA with a similar potency (Figure 4G).

Identification of NS3h inhibitors in Sigma's LOPAC 1280™

To test if a DNA binding assay could be used to identify new HCV helicase inhibitors, the above FP-based assay was used to screen Sigma's 1280-compound LOPAC. All LOPAC compounds were screened at 100 μM in 384-well plates, each containing positive (primuline or dT_{20}) and negative (DMSO or buffer only) controls (Figure 5A). Out of the 1280 samples screened (Table S2), 18 compounds exhibited FP signals significantly different from other library samples. To identify compounds that decreased FP by quenching of the fluorescence signal or intrinsic fluorescence, the fluorescence intensity of each compound (I) was divided by the fluorescence intensity observed for negative controls ($I_{(-)}$). A plot of this data ($I/I_{(-)}$) revealed that four hits increased or decreased the fluorescence intensity by more than 20% in comparison with the negative controls. Four of the compounds with similar fluorescence intensity to that of the negative controls decreased FP by more than 60% at a concentration of 100 μM (Figure 5B). Each of these compounds [ATA (Sigma Cat. #A1895), suramin sodium salt (Sigma Cat. #S2671), NF 023 hydrate (Sigma Cat. #N8652) and tyrphostin AG 538 (Sigma Cat. #T7822)] decreased polarization in a concentration-dependent manner (Figure 5C–F). The IC_{50} values with the four best inhibitors were similar to those seen with titan yellow and lower than those seen with primuline and thioflavine S (Table 1).

To test if compounds that decrease FP of the Cy5-dT15–NS3h complex inhibit the ability of NS3h to unwind DNA, various concentrations of each of the compounds above were added to MBHAs that monitor either DNA or RNA unwinding. Three of the four compounds identified in the LOPAC screen inhibited DNA-based MBHAs (Figure 6B). Those that inhibited the ability of NS3h to unwind DNA also inhibited its activity on an RNA substrate (Table 1).

To determine if compounds that interact with the NS3h–DNA complex might also function as antiviral agents, their ability to inhibit the replication of an HCV subgenomic replicon was tested (46). HCV RNA replication was measured using a reporter system in which a *Renilla* luciferase gene was fused to the 5′-end of the neomycin phosphotransferase gene needed for replicon selection (Figure 6C), so that the cellular levels of *Renilla* luciferase correlated directly with the amount of HCV RNA present in cells (35). After replicon transfection and selection, cells were treated in parallel in two sets of triplicates. One set of cells was used for *Renilla* luciferase assays and the other set was used to determine cell viability using a firefly luciferase-based assay. Three of the four compounds identified in the LOPAC screen inhibited replicon luciferase (Figure 6D), and all four compounds showed little sign of toxicity at a concentration of 25 μM (Figure 6E). Selectivity was estimated by comparing the potency with which the compound inhibits the replicon to its toxicity. By this measure, AG 538 was the most selective because three times more of this compound was needed to reduce viability than was needed to inhibit HCV replication (Table 1).

A similar FP-assay using the *E. coli* SSB

The specificity of the new HCV helicase inhibitors was examined using a counterscreen in which NS3h was substituted with the unrelated *E. coli* SSB (Figure 7A). Like NS3h, SSB increased the FP of Cy5-dT15, but more (~20 nM) SSB was needed to saturate the oligonucleotide with a $K_{0.5}$ of 9.6 ± 2 nM in the presence of 5 nM Cy5-dT15 (Figure 7B). All the compounds that inhibited the Cy5-dT15–NS3h interaction also inhibited the

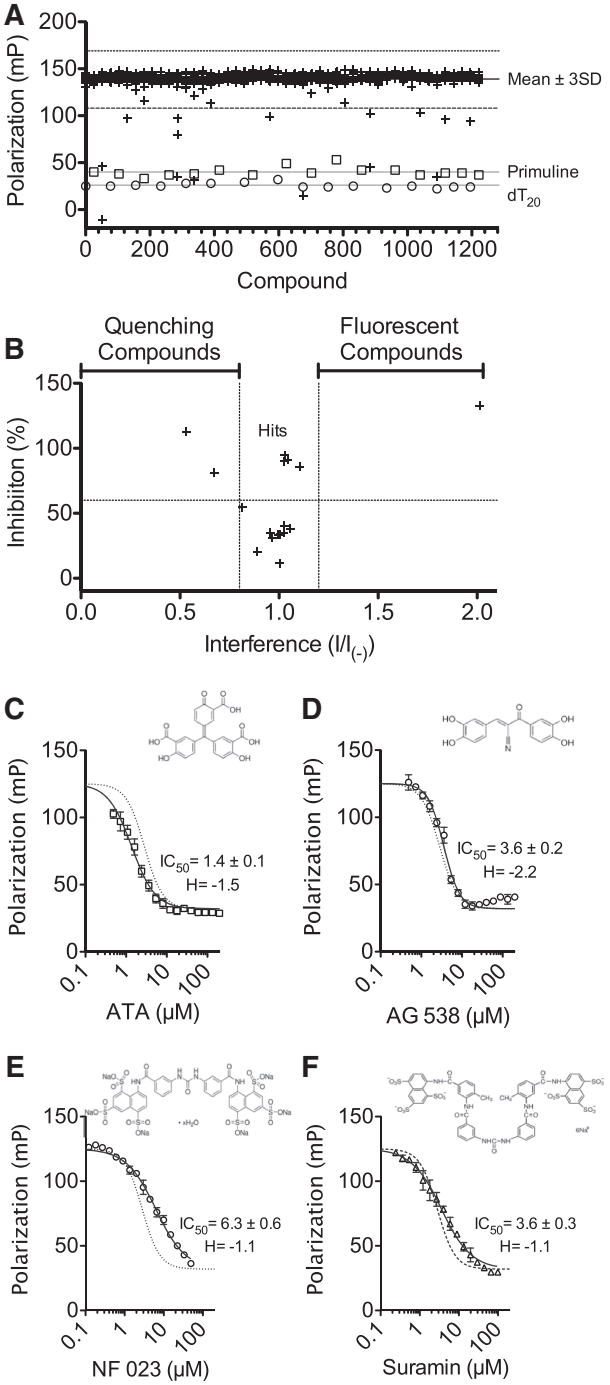

Figure 5. Identification of inhibitors of Cy5-dT15-NS3h complex formation in a screen of the Sigma LOPAC 1280™. (**A**) Summary of screening results of a fluorescence polarization assay to identify inhibitors of the Cy5-dT15-NS3h interaction among the 1280 samples in Sigma's LOPAC (+). Positive controls contained primuline (squares) or dT20 (circles) and negative controls contained DMSO only (not shown). The solid line represents the mean of all assays (except positive controls) and the dotted lines three standard deviations. (**B**) Normalized inhibition (%) for compounds that fall outside the above three standard deviation limit are plotted against the compound interference, defined as fluorescence intensity divided by the average fluorescence intensity of the negative control samples. The vertical dotted lines denote defined boundaries of tolerance for either possible quenching ($I = 0.8$) or possible intrinsic fluorescence ($I = 1.2$). The horizontal dotted line denotes arbitrary cut-off criterion of 60% inhibition. Fluorescence polarization of a Cy5-dT15-NS3h complex in the presence of increasing concentrations of (**C**) ATA, (**D**) AG 538, (**E**) NF 023, or (**F**) Suramin. Data ($n = 3$) were fitted to 4-parameter concentration response curves constrained to values obtained in the absence of inhibitor (top) and the absence of NS3h (bottom) with parameters in Table 1. In (C)–(F), concentration response curve for titan yellow is shown for comparison (dotted lines). Raw data for all LOPAC samples can be found in Table S2.

interaction between Cy5-dT15 and SSB (Figure 7C and Table 1). The specificity of each compound was judged by comparing the IC_{50} values obtained with NS3h and SSB. By this measure, none of the new HCV helicase inhibitors were more specific than the yellow dyes (Table 1).

The yellow dyes were therefore selected to probe if the SSB based counter screen could be used to identify specific HCV helicase inhibitors. Thioflavine S was discovered to inhibit HCV helicase in an MBHA-based screen of the NCI Mechanistic Set of compounds (Figure 8). Li *et al.* (21) isolated eight compounds from thioflavine S and the related dye primuline and used the core dimeric benzothiazole scaffold found in all eight components to synthesize a library of semi-synthetic primuline derivatives. Since we showed above that primuline inhibits NS3h from binding DNA in a non-specific manner, we screened the entire primuline derivative collection for compounds that might be more specific. To this end, we compared the ability of the compounds synthesized from the main component of primuline to disrupt the Cy5-dT15–SSB complex with their ability to inhibit the HCV helicase in a standard HCV helicase MBHA (Figure 8 and Table S3). This structure activity relationship reveals that small changes to this scaffold can affect the affinity of a compound for HCV helicase relative to its ability to inhibit SSB from binding DNA. The most potent and specific compound in this family, CID50930730, is over 30 times more specific (as judged by the ratio of IC_{50} values for each compound in the MBHA to its IC_{50} value in SSB-DNA binding assays, for each compound) than the least specific compound with similar potency in the MBHA, CID49849276 (Figure 8 and Table S3).

DISCUSSION

This study shows how DNA-binding assays can be used to discover and characterize small molecules that inhibit helicases. The assays are simpler than those used to monitor helicase-catalyzed DNA unwinding or ATP hydrolysis, making them more amenable to high throughput screening (HTS). Despite its simplicity, the FP-based DNA binding assay developed here was able to find four compounds that disrupt the HCV helicase-DNA interaction, three of which also inhibit the NS3h's ability to unwind DNA and RNA. Three compounds also inhibit replication of subgenomic HCV replicons. Similar binding assays using unrelated protein SSB were shown to be useful for judging compound specificity, as was demonstrated both with the newly identified helicase inhibitors and with a panel of compounds created in a prior SAR study of the primuline scaffold (21).

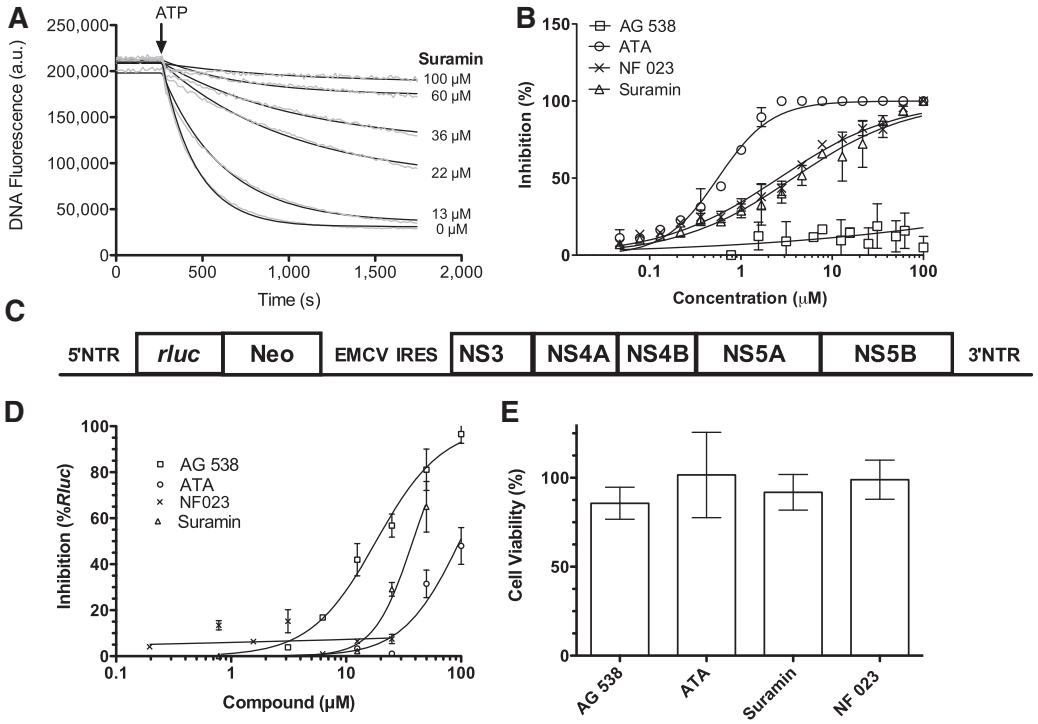

Figure 6. Ability of compounds that disrupt the Cy5-dT15-NS3h complex to inhibit the HCV helicase and HCV replication. (**A**) Fluorescence intensity of the MBHA substrate in assays containing increasing concentrations of suramin. (**B**) Effect of AG 538 (squares), ATA (circles), NF 023 (x), and suramin (triangles) on the initial rates of HCV helicase catalyzed DNA unwinding. Points are means of duplicate reactions, and error bars are standard deviations. Data are fit to a normalized concentration response equation with parameters listed in Table 1. (**C**) The sub-genomic *Renilla* luciferase reporter replicon used to monitor compound effects on HCV replication. (**D**) Relative HCV RNA levels in the presence of various concentrations of AG 538 (squares), ATA (circles), NF 023 (x), and Suramin (triangles). Data are fit to a normalized concentration response equation with parameters in Table 1. (**E**) Average (±SD) cell viability in assays where cells were exposed to 25 μM of indicated compounds.

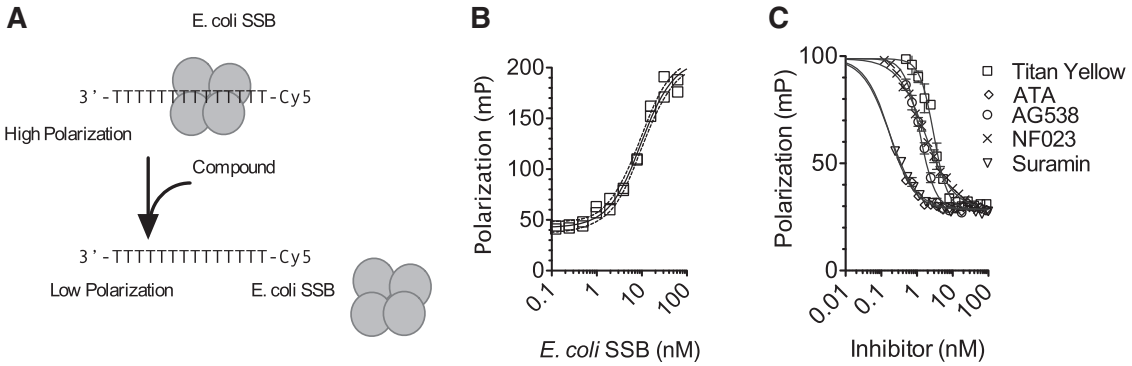

Figure 7. Effect of compounds on the polarization of a Cy5-dT15-*Escherichia coli* single-stranded DNA binding protein (SSB) complex. (**A**) FP based assay to monitor SSB binding to Cy5-dT15. (**B**) Binding between Cy5-dT15 and SSB determined by FP. (**C**) Cy-dT15-SSB complexes were titrated with titan yellow (squares), ATA (diamonds), NF 023 (x), AG 538 (circles) or Suramin (inverted triangles). Assays were performed in triplicate, points show means, and error bars standard deviations. Data are fit to a 4-parameter concentration equation constrained to values obtained in the absence of inhibitor (top) and the absence of SSB (bottom).

The interaction of HCV NS3 helicase with ssDNA was monitored here with four different assays. The first, gel shift analysis, is probably the most common method used to study protein nucleic acid interactions. The gel shift assay is laborious, not readily amenable to automation, and requires relatively large amounts of DNA and protein. Of the three HTS compatible methods evaluated, the FP-based method was the most precise, reproducible and cost effective. FP-based assays have been used before to measure the binding of helicases to a labeled substrate (40,41), but have not been previously reported as methods to screen for HCV helicase inhibitors. DNA binding to NS3h can also be monitored either by measuring intrinsic protein fluorescence (30,31) or by monitoring changes in the fluorescence intensity of a fluorescein-labeled oligonucleotide when it binds NS3h (9). Monitoring intrinsic

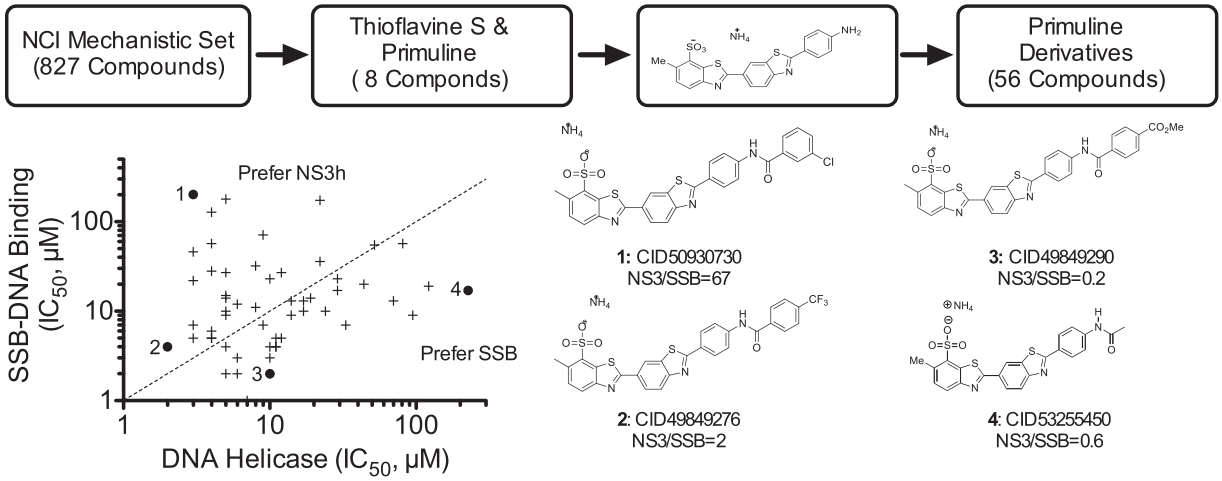

Figure 8. Synthesis of specific HCV helicase inhibitors from a scaffold isolated from the yellow dye primuline. The flow chart summaries the source of compounds tested (see text for details). The plot shows the ability of various primuline derivatives to inhibit HCV helicase (*x*-axis) and decrease polarization of a Cy5-dT15-SSB complex. The dotted line shows where hypothetical compounds that inhibit both assays with the same potency would lie on the plot. Structures of the four compounds with the most extreme properties are shown on the right, along with the ratios of IC_{50} values obtained in the two different assays. All data, structures and CID numbers can be found in Table S3.

protein fluorescence is usually difficult in the presence of small molecules, especially if they absorb light in the ultraviolet wavelengths. Use of fluorescence intensity based assays in screening is also difficult, because many library samples fluoresce in the same range as fluorescein, and as noted above, we have not yet found an alternate red-shifted fluorophore that changes intensity when it interacts with NS3h.

The LOPAC samples that most potently disrupted the NS3h–DNA complex were two polysulfonated naphthylureas (suramin and NF 023), a triphenylmethane (ATA) and a tyrphostin (AG 538). All but the tyrphostin inhibit helicase catalyzed strand separations. Tyrphostin AG 538 mimics a tyrosine kinase substrate so that it acts as a competitive inhibitor of the IGF-1 receptor tyrosine kinase (47). Preliminary mechanistic studies on each compound suggest that only ATA inhibits the ability of NS3h to cleave ATP in the absence of DNA or RNA, and all but AG 538 prevent RNA from stimulating ATP hydrolysis. Similarly, gel shift assays show all but AG 538 displace NS3h from DNA, as was seen with thioflavine S (Figure 1B). These data suggest that the AG 538 induced decrease in the polarization of both NS3h–Cy5-dT15 and SSB–Cy5-dT15 complexes might be due to a fluorescence artifact or something other than the ability of the tyrphostin to prevent protein from binding DNA. The ability of AG 538 to inhibit growth of the HCV replicon is likewise probably not due to its effects on NS3. AG 538 is an inhibitor of the insulin-like growth factor I (IGF-1) tyrosine kinase, and it is possible IGF-1-mediated signaling is needed for efficient HCV replication. Both HCV infection and a reduction of IGF-1 levels are linked to the development of liver cancer (48).

Compounds binding in place of ATP could also cause the helicase to release its grip on DNA in the above binding assay because ATP binding and hydrolysis causes HCV helicase to cycle between low affinity and high affinity DNA-binding states (28). When NS3h releases DNA, it slides from the 3′ to 5′ end of a nucleic acid as a Brownian motor (49). Thus, in light of the recent demonstration that most nucleoside triphosphates can fuel this motor action (6), it is not surprising that 2-methyl-ATP, 2-(methylthio)ATP and 2-chloroATP were also hits in the LOPAC screen. The fact that they inhibited binding by only 30–40% of NS3h (which was less than our arbitrary 60% cutoff) is also not surprising since they were tested at concentrations far less than the concentration of ATP needed to fuel unwinding, or NS3 translocation, at half-maximum rates (6). In contrast, α,β-methylene ATP did not inhibit NS3h from binding dT15 (Table S1), confirming the earlier observations that most of the canonical non-hydrolysable ATP analogs are poor inhibitors of HCV helicase (22,50).

The fact that the polysulfonated naphthylureas and triphenylmethanes affect HCV helicase is noteworthy because the anti-microbial properties of these compounds are well documented. Suramin has long been used to treat sleeping sickness caused by trypanosomes, and it inhibits protein tyrosine phosphatases (51) and G-proteins (52). G-proteins and helicases share a similar Walker-type nucleotide-binding site (52), and it is possible that suramin inhibits HCV helicase and G-proteins through a similar molecular mechanism. NF 023 is a suramin analog, P2X receptor antagonist (53), and inhibitor of RNA editing in trypanosomes (54). Suramin and NF 023 behave similarly in all *in vitro* assays here, but it is noteworthy that (among the two) only suramin was effective against the HCV replicon in cells. A simple explanation would be that the somewhat more aromatic suramin is more likely to enter cells to exert an intracellular effect. Our results also confirm the recently reported antiviral effect of ATA against the HCV replicon, which had been reported after ATA was found to inhibit the HCV NS5B RNA-dependent RNA polymerase (55). ATA exerts a similar

effect against a wide variety of enzymes that manipulate nucleic acids, like human flap endonuclease 1 (FEN1) (56). ATA also inhibits replication of influenzas A and B (57). Triphenylmethanes that resemble ATA have been developed from the dye Soluble Blue HT as HCV helicase inhibitors (14).

This study is focused on finding compounds that inhibit nucleic acids from binding to the known, high affinity-binding site on the NS3 helicase region. To best target this site, we have used truncated NS3 lacking the protease region (i.e. NS3h). Another advantage to using NS3h instead of full length NS3 is that the truncated protein expresses at higher levels in *E. coli* and is more stable after purification. The same assays used here have also been performed with full-length NS3 and NS3–NS4A fusion peptides, with similar results, and it might be possible to perform the screens here with both full-length NS3 and NS3h to identify compounds that target the still poorly defined nucleic acid binding sites on the protease or in the cleft separating the protease from the helicase. Such compounds might simultaneously inhibit both NS3 protease and helicase activities. To date, no small molecules that simultaneously inhibit both the NS3 protease and helicase have been reported in the academic literature, although a recent structure shows that a protease inhibitor can interact with residues in both the helicase and protease domains (58).

In any HTS campaign, it is important to have an appropriate counter screen to identify non-specific compounds. We show here that unrelated DNA binding proteins can be substituted for NS3h in the FP-assay to identify such compounds. The results show that the four LOPAC hits affect both NS3h and *E. coli* SSB non-specifically to inhibit the binding of the two proteins to nucleic acids. As further evidence for a lack of specificity, both suramin and ATA were hits in a LOPAC screen that used a similar assay to identify compounds that prevent the RNA-induced silencing complex from binding to RNA (59). We show here how this SSB-based counterscreen can be used to identify more specific NS3 helicase inhibitors using a library of recently disclosed semi-synthetic analogs of potent helicase inhibitors found in primuline (21). To identify primuline analogs that have a greater affinity for HCV helicase than they do for DNA, Li *et al*. (21) used an assay that monitors the ability of the primuline derivatives to displace SYBR Green I from DNA. As in this study, the most specific derivative in the study by Li *et al*. was CID50930730 (Figure 7D), and the structure activity relationship observed here with the SSB assay (Table S3) essentially mirrors the relationships previously seen with DNA binding data. The one important difference was that less of each compound was needed to inhibit SSB binding than was needed to displace SYBR Green I (21).

In conclusion, we established a new set of tools that can be used to discover and analyze HCV helicase inhibitors. None of these assays are new, and they have been extensively reviewed elsewhere in the context of both DNA (60) and RNA binding proteins (61). While the helicase inhibitors identified from Sigma's LOPAC are not specific for NS3h, screens of larger, more diverse libraries might yield potent, specific probes needed to study the role of HCV helicase in cells. On the other hand, more specific analogs of non-specific screening hits could be synthesized, as was demonstrated above with the primuline derivatives. Screens of the LOPAC and helicase inhibitor libraries show that the binding assays presented here are easier to interpret, and less prone to compound interference, than assays monitoring helicase catalyzed DNA separation.

SUPPLEMENTARY DATA

Supplementary Data are available at NAR Online: Supplementary Tables 1–3.

ACKNOWLEDGEMENTS

We would like to thank Peter Hodder (Scripps Florida) for valuable advice in assay development, and Seng-Lai Tan for providing the HCV replicon.

FUNDING

National Institutes of Health [RO1 AI088001]; Research Growth Initiative Award [101X219] from the University of Wisconsin-Milwaukee Research Foundation; National Institutes of Health Molecular Libraries Initiative [U54 HG005031]. Funding for open access charge: University of Wisconsin-Milwaukee Research Foundation.

Conflict of interest statement. None declared.

REFERENCES

1. Kwong,A.D., Rao,B.G. and Jeang,K.T. (2005) Viral and cellular RNA helicases as antiviral targets. *Nat. Rev. Drug Discov.*, **4**, 845–853.
2. Belon,C.A. and Frick,D.N. (2009) Helicase inhibitors as specifically targeted antiviral therapy for hepatitis C. *Future Virol.*, **4**, 277–293.
3. Crute,J.J., Grygon,C.A., Hargrave,K.D., Simoneau,B., Faucher,A.M., Bolger,G., Kibler,P., Liuzzi,M. and Cordingley,M.G. (2002) Herpes simplex virus helicase-primase inhibitors are active in animal models of human disease. *Nat. Med.*, **8**, 386–391.
4. Kleymann,G., Fischer,R., Betz,U.A., Hendrix,M., Bender,W., Schneider,U., Handke,G., Eckenberg,P., Hewlett,G., Pevzner,V. *et al*. (2002) New helicase-primase inhibitors as drug candidates for the treatment of herpes simplex disease. *Nat. Med.*, **8**, 392–398.
5. Katsumata,K., Chono,K., Sudo,K., Shimizu,Y., Kontani,T. and Suzuki,H. (2011) Effect of ASP2151, a herpesvirus helicase-primase inhibitor, in a guinea pig model of genital herpes. *Molecules*, **16**, 7210–7223.
6. Belon,C.A. and Frick,D.N. (2009) Fuel specificity of the hepatitis C virus NS3 helicase. *J. Mol. Biol.*, **388**, 851–864.
7. Lam,A.M. and Frick,D.N. (2006) Hepatitis C virus subgenomic replicon requires an active NS3 RNA helicase. *J. Virol.*, **80**, 404–411.
8. Stankiewicz-Drogon,A., Dorner,B., Erker,T. and Boguszewska-Chachulska,A.M. (2010) Synthesis of new acridone derivatives, inhibitors of NS3 helicase, which efficiently and specifically inhibit subgenomic HCV replication. *J. Med. Chem.*, **53**, 3117–3126.
9. Frick,D.N., Rypma,R.S., Lam,A.M. and Gu,B. (2004) The nonstructural protein 3 protease/helicase requires an intact protease domain to unwind duplex RNA efficiently. *J. Biol. Chem.*, **279**, 1269–1280.

10. Suzich,J.A., Tamura,J.K., Palmer-Hill,F., Warrener,P., Grakoui,A., Rice,C.M., Feinstone,S.M. and Collett,M.S. (1993) Hepatitis C virus NS3 protein polynucleotide-stimulated nucleoside triphosphatase and comparison with the related pestivirus and flavivirus enzymes. *J. Virol.*, **67**, 6152–6158.
11. Yao,N., Hesson,T., Cable,M., Hong,Z., Kwong,A.D., Le,H.V. and Weber,P.C. (1997) Structure of the hepatitis C virus RNA helicase domain. *Nat. Struct. Biol.*, **4**, 463–467.
12. Frick,D.N. (2007) The hepatitis C virus NS3 protein: a model RNA helicase and potential drug target. *Curr. Issues Mol. Biol.*, **9**, 1–20.
13. Gemma,S., Butini,S., Campiani,G., Brindisi,M., Zanoli,S., Romano,M.P., Tripaldi,P., Savini,L., Fiorini,I., Borrelli,G. *et al.* (2011) Discovery of potent nucleotide-mimicking competitive inhibitors of hepatitis C virus NS3 helicase. *Bioorg. Med. Chem. Lett.*, **21**, 2776–2779.
14. Chen,C.S., Chiou,C.T., Chen,G.S., Chen,S.C., Hu,C.Y., Chi,W.K., Chu,Y.D., Hwang,L.H., Chen,P.J., Chen,D.S. *et al.* (2009) Structure-based discovery of triphenylmethane derivatives as inhibitors of hepatitis C virus helicase. *J. Med. Chem.*, **52**, 2716–2723.
15. Manfroni,G., Paeshuyse,J., Massari,S., Zanoli,S., Gatto,B., Maga,G., Tabarrini,O., Cecchetti,V., Fravolini,A. and Neyts,J. (2009) Inhibition of subgenomic hepatitis C virus RNA replication by acridone derivatives: identification of an NS3 helicase inhibitor. *J. Med. Chem.*, **52**, 3354–3365.
16. Krawczyk,M., Wasowska-Lukawska,M., Oszczapowicz,I. and Boguszewska-Chachulska,A.M. (2009) Amidinoanthracyclines—a new group of potential anti-hepatitis C virus compounds. *Biol. Chem.*, **390**, 351–360.
17. Najda-Bernatowicz,A., Krawczyk,M., Stankiewicz-Drogon,A., Bretner,M. and Boguszewska-Chachulska,A.M. (2010) Studies on the anti-hepatitis C virus activity of newly synthesized tropolone derivatives: identification of NS3 helicase inhibitors that specifically inhibit subgenomic HCV replication. *Bioorg. Med. Chem.*, **18**, 5129–5136.
18. Phoon,C.W., Ng,P.Y., Ting,A.E., Yeo,S.L. and Sim,M.M. (2001) Biological evaluation of hepatitis C virus helicase inhibitors. *Bioorg. Med. Chem. Lett.*, **11**, 1647–1650.
19. Belon,C.A., High,Y.D., Lin,T.I., Pauwels,F. and Frick,D.N. (2010) Mechanism and specificity of a symmetrical benzimidazolephenylcarboxamide helicase inhibitor. *Biochemistry*, **49**, 1822–1832.
20. Tunitskaya,V.L., Mukovnya,A.V., Ivanov,A.A., Gromyko,A.V., Ivanov,A.V., Streltsov,S.A., Zhuze,A.L. and Kochetkov,S.N. (2011) Inhibition of the helicase activity of the HCV NS3 protein by symmetrical dimeric bis-benzimidazoles. *Bioorg. Med. Chem. Lett.*, **21**, 5331–5335.
21. Li,K., Frankowski,K.J., Belon,C.A., Neuenswander,B., Ndjomou,J., Hanson,A.M., Shanahan,M.A., Schoenen,F.J., Blagg,B.S., Aube,J. *et al.* (2012) Optimization of potent hepatitis C virus NS3 helicase inhibitors isolated from the yellow dyes thioflavine S and primuline. *J. Med. Chem.*, **55**, 3319–3330.
22. Belon,C.A. and Frick,D.N. (2008) Monitoring helicase activity with molecular beacons. *BioTechniques*, **45**, 433–440, 442.
23. Wang,Y., Xiao,J., Suzek,T.O., Zhang,J., Wang,J., Zhou,Z., Han,L., Karapetyan,K., Dracheva,S., Shoemaker,B.A. *et al.* (2012) PubChem's bioAssay database. *Nucleic Acids Res.*, **40**, D400–D412.
24. Belon,C.A. and Frick,D.N. (2011) NS3 helicase inhibitors. In: He,Y. and Tan,S.L. (eds), *Hepatitis C: Antiviral Drug Discovery and Development*. Caister Academic Press, Norfolk, UK, pp. 327–356.
25. Tai,C.L., Chi,W.K., Chen,D.S. and Hwang,L.H. (1996) The helicase activity associated with hepatitis C virus nonstructural protein 3 (NS3). *J. Virol.*, **70**, 8477–8484.
26. Kim,J.L., Morgenstern,K.A., Griffith,J.P., Dwyer,M.D., Thomson,J.A., Murcko,M.A., Lin,C. and Caron,P.R. (1998) Hepatitis C virus NS3 RNA helicase domain with a bound oligonucleotide: the crystal structure provides insights into the mode of unwinding. *Structure*, **6**, 89–100.
27. Mackintosh,S.G., Lu,J.Z., Jordan,J.B., Harrison,M.K., Sikora,B., Sharma,S.D., Cameron,C.E., Raney,K.D. and Sakon,J. (2006) Structural and biological identification of residues on the surface of NS3 helicase required for optimal replication of the hepatitis C virus. *J. Biol. Chem.*, **281**, 3528–3535.
28. Gu,M. and Rice,C.M. (2010) Three conformational snapshots of the hepatitis C virus NS3 helicase reveal a ratchet translocation mechanism. *Proc. Natl. Acad. Sci. USA*, **107**, 521–528.
29. Appleby,T.C., Anderson,R., Fedorova,O., Pyle,A.M., Wang,R., Liu,X., Brendza,K.M. and Somoza,J.R. (2011) Visualizing ATP-dependent RNA translocation by the NS3 helicase from HCV. *J. Mol. Biol.*, **405**, 1139–1153.
30. Preugschat,F., Averett,D.R., Clarke,B.E. and Porter,D.J. (1996) A steady-state and pre-steady-state kinetic analysis of the NTPase activity associated with the hepatitis C virus NS3 helicase domain. *J. Biol. Chem.*, **271**, 24449–24457.
31. Levin,M.K. and Patel,S.S. (2002) Helicase from hepatitis C virus, energetics of DNA binding. *J. Biol. Chem.*, **277**, 29377–29385.
32. Lam,A.M., Keeney,D., Eckert,P.Q. and Frick,D.N. (2003) Hepatitis C virus NS3 ATPases/helicases from different genotypes exhibit variations in enzymatic properties. *J. Virol.*, **77**, 3950–3961.
33. Beran,R.K., Serebrov,V. and Pyle,A.M. (2007) The serine protease domain of hepatitis C viral NS3 activates RNA helicase activity by promoting the binding of RNA substrate. *J. Biol. Chem.*, **282**, 34913–34920.
34. Ray,U. and Das,S. (2011) Interplay between NS3 protease and human La protein regulates translation-replication switch of Hepatitis C virus. *Sci. Rep.*, **1**, 1–8.
35. Huang,Y., Chen,X.C., Konduri,M., Fomina,N., Lu,J., Jin,L., Kolykhalov,A. and Tan,S.L. (2006) Mechanistic link between the anti-HCV effect of interferon gamma and control of viral replication by a Ras-MAPK signaling cascade. *Hepatology*, **43**, 81–90.
36. Belon,C. and Frick,D.N. (2010) Thioflavin S inhibits hepatitis C virus RNA replication and the viral helicase with a novel mechanism. *FASEB J.*, **24**, lb202.
37. Yon,C., Viswanathan,P., Rossignol,J.F. and Korba,B. (2011) Mutations in HCV non-structural genes do not contribute to resistance to nitazoxanide in replicon-containing cells. *Antiviral Res.*, **91**, 233–240.
38. Horobin,R.W., Kiernan,J.A. and Conn,H.J. (2002) *Conn's Biological Stains: A Handbook of Dyes, Stains and Fluorochromes for Use in Biology and Medicine*. BIOS, Oxford, pp. 357–358.
39. Morris,P.D., Byrd,A.K., Tackett,A.J., Cameron,C.E., Tanega,P., Ott,R., Fanning,E. and Raney,K.D. (2002) Hepatitis C virus NS3 and simian virus 40 T antigen helicases displace streptavidin from 5′-biotinylated oligonucleotides but not from 3′-biotinylated oligonucleotides: evidence for directional bias in translocation on single-stranded DNA. *Biochemistry*, **41**, 2372–2378.
40. Tackett,A.J., Corey,D.R. and Raney,K.D. (2002) Non-Watson-Crick interactions between PNA and DNA inhibit the ATPase activity of bacteriophage T4 Dda helicase. *Nucleic Acids Res.*, **30**, 950–957.
41. Xu,H.Q., Zhang,A.H., Auclair,C. and Xi,X.G. (2003) Simultaneously monitoring DNA binding and helicase-catalyzed DNA unwinding by fluorescence polarization. *Nucleic Acids Res.*, **31**, e70.
42. Frick,D.N., Banik,S. and Rypma,R.S. (2007) Role of divalent metal cations in ATP hydrolysis catalyzed by the hepatitis C virus NS3 helicase: magnesium provides a bridge for ATP to fuel unwinding. *J. Mol. Biol.*, **365**, 1017–1032.
43. Zhang,J.H., Chung,T.D. and Oldenburg,K.R. (1999) A Simple Statistical Parameter for Use in Evaluation and Validation of High Throughput Screening Assays. *J. Biomol. Screen.*, **4**, 67–73.
44. Tyagi,S. and Kramer,F.R. (1996) Molecular beacons: probes that fluoresce upon hybridization. *Nat. Biotechnol.*, **14**, 303–308.
45. Boger,D.L. and Tse,W.C. (2001) Thiazole orange as the fluorescent intercalator in a high resolution fid assay for determining DNA binding affinity and sequence selectivity of small molecules. *Bioorg. Med. Chem.*, **9**, 2511–2518.
46. Lohmann,V., Korner,F., Koch,J., Herian,U., Theilmann,L. and Bartenschlager,R. (1999) Replication of subgenomic hepatitis C virus RNAs in a hepatoma cell line. *Science*, **285**, 110–113.
47. Blum,G., Gazit,A. and Levitzki,A. (2000) Substrate competitive inhibitors of IGF-1 receptor kinase. *Biochemistry*, **39**, 15705–15712.

48. Mazziotti,G., Sorvillo,F., Morisco,F., Carbone,A., Rotondi,M., Stornaiuolo,G., Precone,D.F., Cioffi,M., Gaeta,G.B., Caporaso,N. *et al*. (2002) Serum insulin-like growth factor I evaluation as a useful tool for predicting the risk of developing hepatocellular carcinoma in patients with hepatitis C virus-related cirrhosis: a prospective study. *Cancer*, **95**, 2539–2545.
49. Levin,M.K., Gurjar,M. and Patel,S.S. (2005) A Brownian motor mechanism of translocation and strand separation by hepatitis C virus helicase. *Nat. Struct. Mol. Biol.*, **12**, 429–435.
50. Levin,M.K., Gurjar,M.M. and Patel,S.S. (2003) ATP binding modulates the nucleic acid affinity of hepatitis C virus helicase. *J. Biol. Chem.*, **278**, 23311–23316.
51. Zhang,Y.L., Keng,Y.F., Zhao,Y., Wu,L. and Zhang,Z.Y. (1998) Suramin is an active site-directed, reversible, and tight-binding inhibitor of protein-tyrosine phosphatases. *J. Biol. Chem.*, **273**, 12281–12287.
52. Leipe,D.D., Wolf,Y.I., Koonin,E.V. and Aravind,L. (2002) Classification and evolution of P-loop GTPases and related ATPases. *J. Mol. Biol.*, **317**, 41–72.
53. Soto,F., Lambrecht,G., Nickel,P., Stuhmer,W. and Busch,A.E. (1999) Antagonistic properties of the suramin analogue NF023 at heterologously expressed P2X receptors. *Neuropharmacology*, **38**, 141–149.
54. Liang,S. and Connell,G.J. (2010) Identification of specific inhibitors for a trypanosomatid RNA editing reaction. *RNA*, **16**, 2435–2441.
55. Chen,Y., Bopda-Waffo,A., Basu,A., Krishnan,R., Silberstein,E., Taylor,D.R., Talele,T.T., Arora,P. and Kaushik-Basu,N. (2009) Characterization of aurintricarboxylic acid as a potent hepatitis C virus replicase inhibitor. *Antivir. Chem. Chemother.*, **20**, 19–36.
56. Dorjsuren,D., Kim,D., Maloney,D.J., Wilson,D.M. III and Simeonov,A. (2011) Complementary non-radioactive assays for investigation of human flap endonuclease 1 activity. *Nucleic Acids Res.*, **39**, e11.
57. Hashem,A.M., Flaman,A.S., Farnsworth,A., Brown,E.G., Van Domselaar,G., He,R. and Li,X. (2009) Aurintricarboxylic acid is a potent inhibitor of influenza A and B virus neuraminidases. *PLoS ONE*, **4**, e8350.
58. Schiering,N., D'Arcy,A., Villard,F., Simic,O., Kamke,M., Monnet,G., Hassiepen,U., Svergun,D.I., Pulfer,R., Eder,J. *et al*. (2011) A macrocyclic HCV NS3/4A protease inhibitor interacts with protease and helicase residues in the complex with its full-length target. *Proc. Natl. Acad. Sci. USA*, **108**, 21052–21056.
59. Tan,G.S., Chiu,C.H., Garchow,B.G., Metzler,D., Diamond,S.L. and Kiriakidou,M. (2012) Small molecule inhibition of RISC loading. *ACS Chem. Biol.*, **7**, 403–410.
60. Anderson,B.J., Larkin,C., Guja,K. and Schildbach,J.F. (2008) Using fluorophore-labeled oligonucleotides to measure affinities of protein-DNA interactions. *Methods Enzymol.*, **450**, 253–272.
61. Pagano,J.M., Clingman,C.C. and Ryder,S.P. (2011) Quantitative approaches to monitor protein-nucleic acid interactions using fluorescent probes. *RNA*, **17**, 14–20.